10.1515/astro-2017-0110

Baltic Astronomy, vol. 25, 53–59, 2016

STÄCKEL-TYPE DYNAMIC MODEL OF THE GALAXY BASED ON MASER KINEMATIC DATA

A. O. Gromov[1], I. I. Nikiforov[2] and L. P. Ossipkov[†1]

[1] *Department of Space Technologies and Applied Astrodynamics, St. Petersburg State University, Universitetskij pr. 35, Staryj Peterhof, St. Petersburg 198504, Russia; granat08@yandex.ru*

[2] *Department of Celestial Mechanics, St. Petersburg State University, Universitetskij pr. 28, Staryj Peterhof, St. Petersburg 198504, Russia; nii@astro.spbu.ru*

Received: 2016 January 14; accepted: 2016 March 4

Abstract. A dynamic model of the Galaxy is constructed based on kinematic data for masers with trigonometric parallaxes. Maser data is used to compute the model potential in the Galactic plane. The potential is then generalized to three dimensions assuming the existence of a third quadratic integral of motion. The resulting Galactic model potential is of Stäckel's type. The corresponding space density function is determined from Poisson's equation.

Key words: methods: analytical – Galaxy: kinematics and dynamics

1. INTRODUCTION

Constructing models for the Galaxy that are based on the data for masers with trigonometric parallaxes is a popular direction of research (e.g., Reid et al. 2009, 2014; Bajkova & Bobylev 2015; Nikiforov & Veselova 2015). The main advantage of trigonometric parallaxes is that they determine *absolute* (geometric) distances to objects with no assumptions about the distance scale, luminosity calibration, extinction, metallicity, etc. The possibilities for *accurate* VLBI measurements of parallaxes even for *distant* masers (see Fig. 5 in Nikiforov & Veselova 2015) make these objects very important tracers for various investigations of the Milky Way, and stimulate their intensive observations (VERA, VLBA, EVN and other projects).

In this paper, we use the data for 103 masers as published by Reid et al. (2014). We convert the maser parallaxes, proper motions, and radial velocities into Galactocentric distances and rotation velocities (see Appendix). In Section 2 and 3 we fit the rotation curves of the one- and two-component model potentials, respectively, to observational data and estimate the model parameters. To generalize the potential to three dimensions, we use the theory of Stäckel's models (Kuzmin 1952, 1956); we then draw equidensities for both model potentials using the model of mass distribution obtained from Poisson's equation (Section 4).

[†] Deceased on August 22nd, 2015.

2. ONE-COMPONENT MODEL

For the one-component model we use the quasi-isothermal potential

$$\Phi(R,0) = \Phi_0^1 \ln\left[1 + \frac{\beta}{w(R)}\right], \tag{1}$$

where $\beta \in [0, +\infty)$ is a structural parameter of the model,

$$w^2(R) = 1 + \kappa^2 R^2, \tag{2}$$

and Φ_0^1 and κ are scale parameters. This potential was proposed by Kuzmin et al. (1986) for spherical systems.

To construct the model for our Galaxy it is necessary to estimate the parameters Φ_0^1, β, and κ. We fit model circular velocities to the observational data on the Milky Way's rotation curve. The formula for circular velocity is

$$\Theta_c^2(R) = -R\frac{\partial \Phi}{\partial R}(R,0). \tag{3}$$

We estimate the model parameters by ordinary least-squares fitting. We minimize the statistic

$$L^2 = \sum_{i=1}^{103} p_i \left[\Theta_c(R_i) - \Theta_i\right]^2, \tag{4}$$

where $\Theta_c(R_i)$ is the model circular velocity at R_i calculated by Eq. (3); Θ_i is the "observed" rotation velocity calculated from the parallax, proper motion, and radial velocity of a maser; $p_i = 1/\sigma^2_{\Theta_i}$ is the weight, and $\sigma^2_{\Theta_i}$ is the measurement error (see Appendix).

We found that L^2 reaches its minimum at $\Phi_0^1 = 295.4 \pm 1.4$ km^2 s^{-2}, $\kappa = 0.4346 \pm 0.0057$ kpc^{-1}, and $q = 0.9002 \pm 0.0014$. The quasi-isothermal model with these parameter values provides the best approximation to observational data.

The left panel in Fig. 1 compares the model rotation curve with observational data. Here the solid curve, dots, and vertical bars show the model velocity curve $\Theta_c(R)$, maser data, and the Θ_i measurement errors, respectively. The mean error of unit weight for this solution is $\sigma \equiv L/\sqrt{N_{\rm free}} = 3.2$. Large $\sigma = \sqrt{\chi^2/\mathrm{DOF}} \gg 1$ means that residuals can not be explained by measurement errors.

Earlier we constructed a similar model by fitting the same model rotation curve to six independent H I data sets. From these data we found $\Phi_0^1 = 258.1 \pm 1.5$ km^2 s^{-2}, $\kappa = 0.3202 \pm 0.0052$ kpc^{-1}, and $q = 1^{+0}_{-0.008}$ (Gromov et al. 2015). It is the limiting case of the quasi-isothermal model, i.e., the so-called Jaffe model. The mean error of unit weight in this case is $\sigma = 2.98$ km s^{-1}. Note that we set the weights for H I data points proportionally to the length of interval of Galactocentric distances $[x_{\min}, x_{\max}]$ covered by the respective data set (see Gromov et al. 2015 and reference therein). Here, $x = R/R_0$ and R_0 is the solar Galactocentric distance. Thus L^2 and σ for H I data are dimensional statistics, whereas the corresponding functions for masers are dimensionless. Fig. 1 compares the rotation curves constructed for maser (the left panel) and H I (the right panel) data.

3. TWO-COMPONENT MODEL

Multi-component models usually agree better with observational data. Furthermore, the Galaxy has a multi-component structure and therefore each compo-

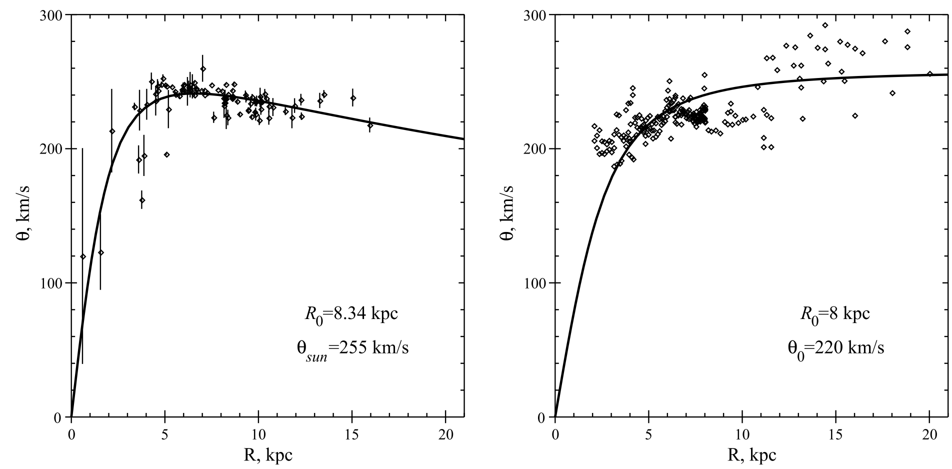

Fig. 1. Comparison of rotation curves for the one-component model constructed for maser (left) and H I (right) data.

nent should be described by its own model potential. We consider a two-component model with the potential

$$\Phi = \Phi_1 + \Phi_2\,, \tag{5}$$

where Φ_1 is quasi-isothermal potential (1) and Φ_2 is the generalized-isochrone potential

$$\Phi_2 = \Phi_0^2 \frac{\alpha}{(\alpha - 1) + \sqrt{1 + \kappa_1^2 R^2}}\,. \tag{6}$$

Minimizing the function L^2 computed for the two-component model applied to maser data yields $\kappa = 0.701{\pm}0.047\,\mathrm{kpc}^{-1}$, $q = 0.99233{\pm}0.00084$, $\Phi_0^1 = 228.0{\pm}1.3$ $\mathrm{km}^2\,\mathrm{s}^{-2}$, $\alpha = 1.41{\pm}0.12$, $\kappa_1 = 0.1467{\pm}0.0055\,\mathrm{kpc}^{-1}$, and $\Phi_0^2 = 178.4{\pm}4.5\,\mathrm{km}^2\,\mathrm{s}^{-2}$. We compare the corresponding rotation curve with observational data in Fig. 2 (the left panel). The mean error of unit weight is $\sigma = 2.8$, i.e., smaller than in the case of the one-component model, and hence the data are better described by the two-component model. However, σ is still much greater than unity.

Our analysis of H I data yields $\kappa = 0.07379{\pm}0.00051\,\mathrm{kpc}^{-1}$, $q = 0.9427{\pm}0.0078$, $\Phi_0^1 = 336.3 \pm 5.9\ \mathrm{km}^2\,\mathrm{s}^{-2}$, $\alpha = 0.403 \pm 0.023$, $\kappa_1 = 0.0574 \pm 0.0037\ \mathrm{kpc}^{-1}$, and $\Phi_0^2 = 288.2 \pm 5.4\ \mathrm{km}^2\,\mathrm{s}^{-2}$ with a mean unit weight error of $\sigma = 2.44\ \mathrm{km\,s}^{-1}$ (Gromov & Nikiforov 2015). We compare the corresponding rotation curve with H I data in Fig. 2 (the right panel).

4. GENERALIZATION OF POTENTIAL TO THREE DIMENSIONS

We use the theory of Stäckel's potentials (Kuzmin 1952, 1956) to generalize the derived potential to three dimensions. We assume that a third integral of motion exists that depends quadratically on velocities:

$$I_3 = (R\,v_z - z\,v_R)^2 + z^2 v_\theta^2 + z_0^2(v_z^2 - 2\Phi^*)\,, \tag{7}$$

where z_0 is a scale parameter of dimension of length, and function $\Phi^*(R,z)$ must

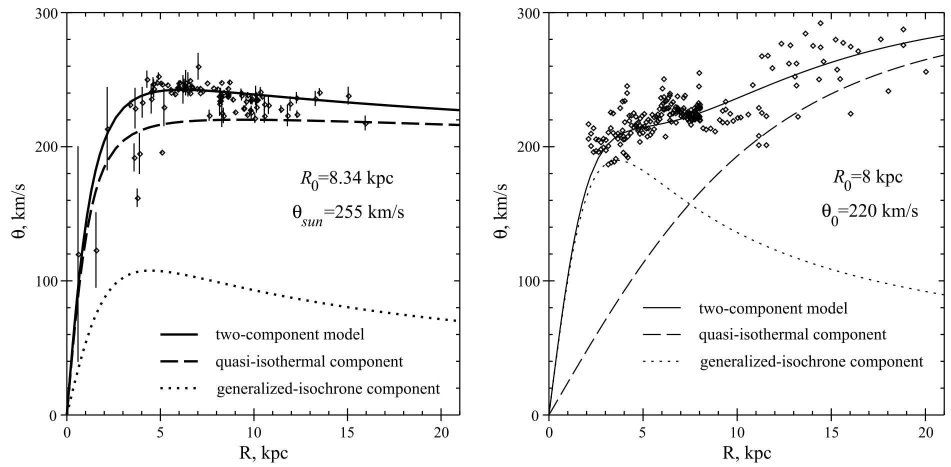

Fig. 2. Comparison of rotation curves for the two-component model constructed from maser (left) and H I (right) data.

satisfy the equations

$$z_0^2 \frac{\partial \Phi^*}{\partial R} = z^2 \frac{\partial \Phi}{\partial R} - Rz \frac{\partial \Phi}{\partial z}\,, \qquad z_0^2 \frac{\partial \Phi^*}{\partial z} = (R^2 + z_0^2) \frac{\partial \Phi}{\partial z} - Rz \frac{\partial \Phi}{\partial R}\,. \tag{8}$$

In the elliptic coordinates $\xi_1 \in [1;\infty)$, $\xi_2 \in [-1;1]$,

$$R = z_0 \sqrt{(\xi_1^2 - 1)\,(1 - \xi_2^2)}\,, \qquad z = z_0\, \xi_1\, \xi_2\,, \tag{9}$$

Stäckel's potentials have the following form:

$$\Phi = \frac{\varphi(\xi_1) - \varphi(\xi_2)}{\xi_1^2 - \xi_2^2}\,, \tag{10}$$

where $\varphi(\xi)$ is an arbitrary function. Determining function $\varphi(\xi)$ for some potential means generalizing this potential to 3D space. To find $\varphi(\xi)$, we use formulas derived by Rodionov (1974).

For our one-component model,

$$\varphi(\xi) = \xi^2 \Phi_0^1 \ln \left(1 + \frac{\beta}{\sqrt{1 + \kappa^2 z_0^2 (\xi^2 - 1)}} \right) \tag{11}$$

(Gromov 2013, 2014a), and for the two-component model,

$$\varphi(\xi) = \xi^2 \Phi_0^1 \ln \left(1 + \frac{\beta}{\sqrt{1 + \kappa^2 z_0^2 (\xi^2 - 1)}} \right) + \\ + \xi^2 \Phi_0^2 \frac{\alpha}{(\alpha - 1)\, \sqrt{1 + \kappa_1^2 z_0^2 (\xi^2 - 1)}} \tag{12}$$

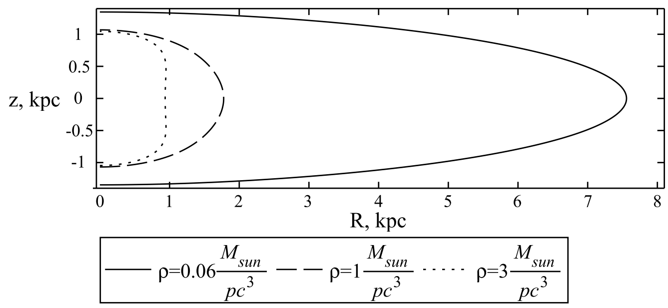

Fig. 3. Density contours for the one-component model based on maser data.

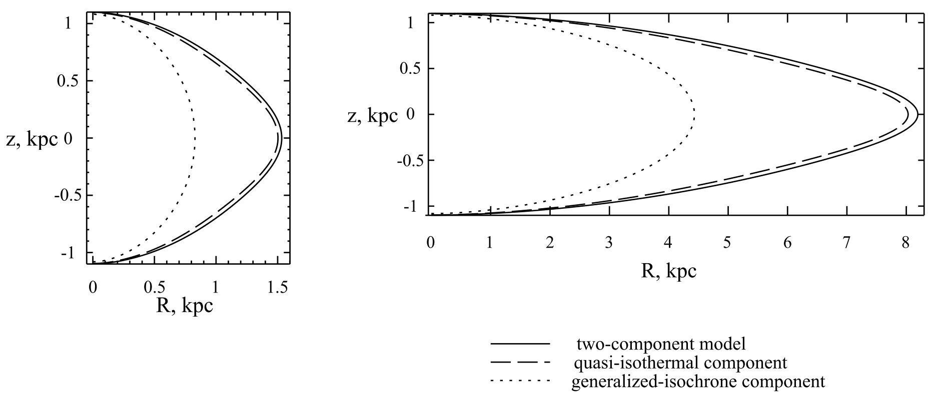

Fig. 4. Density contours for the two-component model based on maser data: $\rho = 1\ M_\odot\,\mathrm{pc}^{-3}$ (left), $\rho = 0.08\ M_\odot\,\mathrm{pc}^{-3}$ (right).

(Gromov 2014b).

We use the spatial density derived from Poisson's equation (Gromov 2013, 2014a,b) to draw the density contours for both models (Figs. 3 and 4). Here we adopt the parameter values inferred from maser data (see Sections 2 and 3). The parameter z_0, which appears in the formula for density, is determined from the following equation:

$$z_0^2(R) = \left[\frac{3\dfrac{\partial\Phi(R,z)}{\partial R} + R\left(\dfrac{\partial^2\Phi(R,z)}{\partial R^2} - 4\dfrac{\partial^2\Phi(R,z)}{\partial z^2}\right)}{\dfrac{\partial^3\Phi(R,z)}{\partial z^2\partial R}}\right]\Bigg|_{z=0} - R^2 \qquad (13)$$

(Ossipkov 1975). Equation (13) is the constraint that the third integral of motion imposes on the potential. We assume that in the solar neighborhood the potential is close to that proposed by Gardner et al. (2011), and substitute the latter into Equation (13). Note that the above authors constructed their potential based on the data on the vertical component of the Galactic tidal field, and we therefore assume that it should describe the vertical structure of our Galaxy quite well. For Gardner et al.'s potential, $z_0 = 5.3$ kpc in the solar neighborhood ($R = 8$ kpc).

5. DISCUSSION AND CONCLUSIONS

We used the observational data for masers to consider the possibility of applying the quasi-isothermal and two-component models (with the quasi-isothermal and generalized-isochrone potentials) to our Galaxy. The models constructed fit the data well. The corresponding unit-weight errors, $\sigma \approx 3 \pm 0.2$, show that a more correct system of weights is needed to eliminate eventual systematic biases. We plan to introduce such a system of weights, although it will complicate the procedure of constructing the model. We also plan to pay attention to the treatment of outlying data.

It follows from a comparison of the results obtained using maser data with those based on H I observations that the parameter q is close to unity. Hence the models are similar to the limiting case, i.e., to the Jaffe model. However, the parameter q for the two-component models does not reach unity, and hence the two-component models are more physical. Such q's result in the elliptical shape of density contours.

We constructed the model of mass distribution by generalizing the potential to 3D space using the theory of Stäckel's potentials. Note that the model density values in the solar neighborhood, $\rho = 0.06\ M_\odot\,\mathrm{pc}^{-3}$, and $0.08\ M_\odot\,\mathrm{pc}^{-3}$ for the one- and two-component models, respectively, are close to the observed density, $\rho = 0.08 - 0.11\ M_\odot\,\mathrm{pc}^{-3}$ (e.g., Loktin & Marsakov 2010).

Physically, it would be natural to construct a three-component model of the Galaxy representing the halo, disk, and bulge. In our two-component model the quasi-isothermal component represents the disk and halo, and the generalized-isochrone component, the bulge.

ACKNOWLEDGMENTS. One of us (IIN) acknowledges the support from Saint Petersburg State University (grant No. 6.37.341.2015).

REFERENCES

Bajkova A. T., Bobylev V. V. 2015, Baltic Astronomy, 24, 43
Gardner E., Nurmi P., Flynn C., Mikkola S. 2011, MNRAS, 411, 947
Gromov A. O. 2013, Izv. Glavn. Astron. Obs. (Pulkovo), 221, 129
Gromov A. O. 2014a, Vest. Saint Petersburg Univ., ser. 1, 2, 322
Gromov A. O. 2014b, Astron. and Astrophys. Trans., 28, 331
Gromov A. O., Nikiforov I. I. 2015, Izv. Glavn. Astron. Obs. (Pulkovo), 222, 31
Gromov A. O., Nikiforov I. I., Ossipkov L. P. 2015, Baltic Astronomy, 24, 150
Kuzmin G. G. 1952, Publ. Tartu Obs., 32, 332
Kuzmin G. G. 1956, AZh, 33, 27
Kuzmin G. G., Veltmann Ü.-I. K., Tenjes P. L. 1986, Publ. Tartu Obs., 51, 232
Loktin A. V., Marsakov V. A. 2010, Lectures on Stellar Astronomy, Rostov-na-Donu, pp. 282 (in Russian)
Nikiforov I. I., Veselova A. V. 2015, Baltic Astronomy, 24, 387
Ossipkov L. P. 1975, Vest. Leningrad Univ., 7, 151
Rodionov V. I. 1974, Vest. Leningrad Univ., 13, 142
Reid M. J., Menten K. M., Zheng X. W. et al. 2009, ApJ, 700, 137
Reid M. J., Menten K. M., Brunthaler A. et al. 2014, ApJ, 793, 72

APPENDIX

We basically follow the procedure outlined by Reid et al. (2009).

1. Conversion of the velocity relative the LSR, $V_{\rm lsr}$, into heliocentric velocity V_r:
$$V_r = V_{\rm lsr} - U_\odot \cos l \cos b - V_\odot \sin l \cos b - W_\odot \sin b\,,$$
where $U_\odot = 10.3\ \mathrm{km\,s^{-1}}$, $V_\odot = 15.3\ \mathrm{km\,s^{-1}}$, $W_\odot = 7.7\ \mathrm{km\,s^{-1}}$, according to a value of 20 $\mathrm{km\,s^{-1}}$ toward $\alpha(1900) = 18^{\rm h}$, $\delta(1900) = +30°$.

2. Conversion of equatorial coordinates (α, δ) into the galactic coordinates (l, b):
$$\sin b = \sin\delta\cos(90° - \delta_{\rm p}) - \cos\delta\sin(\alpha - \alpha_{\rm p} - 6^{\rm h})\sin(90° - \delta_{\rm p})\,,$$
$$\sin\varphi = \left[\cos\delta\sin(\alpha - \alpha_{\rm p} - 6^{\rm h})\cos(90° - \delta_{\rm p}) + \sin\delta\sin(90° - \delta_{\rm p})\right] / \cos b\,,$$
$$\cos\varphi = \cos\delta\cos(\alpha - \alpha_{\rm p} - 6^{\rm h}) / \cos b\,, \qquad l = \varphi + (\theta - 90°)\,,$$
where $\alpha_{\rm p} = 12^{\rm h}51^{\rm m}26\overset{\rm s}{.}2817$, $\delta_{\rm p} = 27°07'42\overset{''}{.}013$, $\theta = 122\overset{\circ}{.}932$

3. Conversion of the proper-motion components in equatorial coordinates (μ_α, μ_δ) into the motion components in Galactic coordinates (μ_l, μ_b):
$$\mu_l = l(\alpha + \mu_\alpha, \delta + \mu_\delta) - l(\alpha, \delta)\,, \qquad \mu_b = b(\alpha + \mu_\alpha, \delta + \mu_\delta) - b(\alpha, \delta)\,.$$

4. The calculation of the velocity components:
$$V_l = k\, r \mu_l \cos b\,, \qquad V_b = k\, r \mu_b\,,$$
where $k = 4.7406$.

5. Conversion to the Cartesian heliocentric coordinate system:
$$U = (V_r \cos b - V_b \sin b)\cos l - V_l \sin l,$$
$$V = (V_r \cos b - V_b \sin b)\sin l + V_l \cos l,$$
$$W = V_b \cos b + V_r \sin b.$$

6. Conversion to the Galactocentric coordinate system associated with the Sun:
$$U_{\rm g} = U + U_\odot\,, \qquad V_{\rm g} = V + \theta_\odot\,, \qquad W_{\rm g} = W + W_\odot\,,$$
where $U_\odot = 11\ \mathrm{km\,s^{-1}}$, $\theta_\odot = 255\ \mathrm{km\,s^{-1}}$, $W_\odot = 9\ \mathrm{km\,s^{-1}}$ (Reid et al. 2014).

7. Conversion in the Galactocentric coordinate system associated with the object:
$$R^2 = R_0^2 + r^2\cos^2 b - 2R_0 r\cos l\cos b, \qquad \Theta = V_{\rm g}\cos\beta + U_{\rm g}\sin\beta,$$
$$\sin\beta = \frac{r\cos\beta}{R}\sin l, \qquad \cos\beta = \frac{R_0 - r\cos b\cos l}{R}\,,$$
where $R_0 = 8.34$ kpc (Reid et al. 2014).

8. The measurement error in Θ is
$$\sigma_\Theta^2 = \left(\frac{\partial\Theta}{\partial\pi}\right)^2\sigma_\pi^2 + \left(\frac{\partial\Theta}{\partial\mu_\alpha}\right)^2\sigma_{\mu_\alpha}^2 + \left(\frac{\partial\Theta}{\partial\mu_\delta}\right)^2\sigma_{\mu_\delta}^2 + \left(\frac{\partial\Theta}{\partial V_r}\right)^2\sigma_{{\rm V}_r}^2\,,$$
where the measurement errors σ_π, σ_{μ_α}, σ_{μ_δ}, $\sigma_{{\rm V}_r}$ are adopted from Reid et al. (2014).